Multi-proxy approach for studying the foraging habitat and trophic position of a migratory marine consumer in the southwestern Atlantic Ocean

Juliano L. Coletto[1,2,*], Alexi C. Besser[3], Silvina Botta[2,4], Lauro A. S. P. Madureira[1,2], Seth D. Newsome[3]

[1]Laboratório de Tecnologia Pesqueira e Hidroacústica, Instituto de Oceanografia, Universidade Federal do Rio Grande (FURG), Rio Grande, RS 96203-900, Brazil
[2]Programa de Pós-Graduação em Oceanografia Biológica, Instituto de Oceanografia, Universidade Federal do Rio Grande (FURG), Rio Grande, RS 96203-900, Brazil
[3]Department of Biology, University of New Mexico, Albuquerque, NM 87131, USA
[4]Laboratório de Ecologia e Conservação da Megafauna Marinha, Instituto de Oceanografia, Universidade Federal do Rio Grande (FURG), Rio Grande, RS 96203-900, Brazil

ABSTRACT: Skipjack tuna *Katsuwonus pelamis* sustains the largest catches among tuna species. Despite its relevance for global food security and the tuna canning industry, information about its foraging ecology in the southwestern Atlantic Ocean (SWAO) is limited. We combined amino acid (AA) and bulk tissue nitrogen isotope ($\delta^{15}N$) analysis with stomach content analysis (SCA) to study skipjack foraging habitat and trophic position (TP) in the SWAO. Mean ($\pm$SD) $\delta^{15}N$ values of source AAs lysine (Lys: 6.5 ± 1.3‰) and phenylalanine (Phe: 10.6 ± 1.3‰) were higher at higher latitudes (30–34° S) of the southern area relative to the northern area between 20–26° S (Lys: 3.4 ± 1.1‰, Phe: 8.2 ± 1.2‰). Correlations between bulk tissue $\delta^{15}N$ ($\delta^{15}N_{bulk}$) and source AA $\delta^{15}N$ showed that Lys is a more robust indicator of $\delta^{15}N$ baseline variation in this region than Phe. Regional mixing models based on AA $\delta^{15}N$ indicated spatial structure in foraging habitat: smaller individuals use the southern area and larger individuals forage at lower latitudes or in offshore areas. TP estimates using the Glx-Lys trophic-source AA pair were in much better agreement with TP estimates based on SCA (TP_{SCA}) and on bulk tissue analysis (TP_{bulk}) than those using Glx-Phe. Skipjack forages across multiple food webs throughout its lifecycle in the SWAO and increases its TP with ontogeny ($TP_{Glx-Lys}$: 3.5–4.0). Stock management strategies should consider that the southern region supports dense aggregations of juvenile skipjack, which may be more vulnerable to non-selective fisheries.

KEY WORDS: Foraging ecology · Movement · AA-CSIA · Stable isotopes · Nitrogen · Amino acids · *Katsuwonus pelamis*

1. INTRODUCTION

Skipjack tuna *Katsuwonus pelamis* (Scombridae) (hereafter 'skipjack') sustain the largest commercial catches among tunas, ranking third among marine fish resources harvested by global fisheries (FAO 2020). The species forms large schools in tropical and subtropical areas of the Atlantic, Indian, and Pacific Oceans (Colette & Nauen 1983). Despite its global distribution and economic importance, skipjack movement patterns are poorly resolved due to its relatively small body size, which limits the use of satellite tags to study movement patterns over the range of sizes harvested by fisheries. In addition, tagging

only tracks movement and cannot resolve foraging habits. Foraging can be addressed by the use of complementary techniques like stomach content analysis (SCA) and stable isotope analysis (SIA) to study ontogenetic patterns in diet composition and trophic positions (TPs) of top predators in pelagic food webs (Popp et al. 2007, Pethybridge et al. 2018, Le-Alvarado et al. 2021).

Nitrogen isotope ($\delta^{15}N$) analysis is often used to estimate TP and food chain length due to systematic increases of ~2–4‰ in $\delta^{15}N$ values between consumers and their prey (DeNiro & Epstein 1981, Minagawa & Wada 1984, Peterson & Fry 1987, Post 2002). A frequent complicating factor in interpreting $\delta^{15}N$ values of top consumers is that $\delta^{15}N$ values of primary producers at the base of food webs can vary spatially as a function of taxonomy, inorganic nitrogen source (e.g. N_2, nitrate, ammonia), and the efficiency with which nitrogen sources are utilized (Sigman et al. 2009, Graham et al. 2010, McMahon et al. 2013, Trueman & Glew 2019). Thus, interpreting bulk tissue $\delta^{15}N$ values ($\delta^{15}N_{bulk}$) is complicated by the potential effects of changes in TP and variations in the isotope values of primary producers that fuel pelagic marine food webs (Graham et al. 2010, McMahon & Newsome 2019).

Compound-specific SIA (CSIA) of individual amino acids (AA) allows one to separate changes caused by variation in baseline $\delta^{15}N$ values from those related to changes in consumer TP (Popp et al. 2007). Trophic AAs (e.g. glutamic acid [Glx], proline [Pro]) undergo significant ^{15}N-enrichment during trophic transfer, while source AAs (e.g. phenylalanine [Phe], lysine [Lys]) experience minimal isotopic alteration as they are passed from prey to consumer (McClelland & Montoya 2002, Popp et al. 2007, McMahon & McCarthy 2016, McMahon & Newsome 2019). This method can be particularly useful for studying the trophic ecology of migratory tunas, which may shift their diet (i.e. TP) and/or foraging areas with ontogeny (e.g. Popp et al. 2007, Graham et al. 2010, Madigan et al. 2014, 2016, Le-Alvarado et al. 2021, Médieu et al. 2021).

Phe has been the preferred source AA and proxy for baseline $\delta^{15}N$ values (Lorrain et al. 2015, Le-Alvarado et al. 2021). Recent studies have shown that $\delta^{15}N_{Phe}$ values of yellowfin tuna *Thunnus albacares* muscle are correlated with $\delta^{15}N$ values in primary producers (i.e. particulate organic matter) and primary consumers (e.g. copepods, barnacles) in the Indian and Pacific Oceans (Popp et al. 2007, Lorrain et al. 2015) and the Gulf of Mexico (Le-Alvarado et al. 2021). However, TP estimates using Phe as the

source AA were a full trophic level lower than expected for yellowfin tuna (Bradley et al. 2015, Lorrain et al. 2015). In addition, a feeding experiment on captive Pacific bluefin tuna *T. orientalis* by Bradley et al. (2014) reported significant consumer-diet $\delta^{15}N$ offsets for Phe (1.5 ± 0.3‰) but negligible offset for Lys (−0.3 ± 0.4‰). These findings suggest Lys may be a promising source AA for studying $\delta^{15}N$ baseline patterns and the trophic ecology of tuna and other top marine consumers (Bradley et al. 2014, McMahon & Newsome 2019).

The distinct oceanographic regimes between the northern (20–28°S) and southern (28–34°S) areas of skipjack feeding grounds in the southwestern Atlantic Ocean (SWAO) result in spatial patterns in zooplankton $\delta^{15}N$ isoscapes (Troina et al. 2020a), making it an ideal system for the use of AA $\delta^{15}N$-based TP studies. Lower baseline $\delta^{15}N$ values in the northern area indicate a substantial contribution of a ^{15}N-depleted inorganic nitrogen source to the oligotrophic waters of the Brazil Current (BC), in which diazotrophic cyanobacteria (e.g. *Trichodesmium*) perform N_2 fixation, resulting in characteristically low $\delta^{15}N$ values (Sigman et al. 2009, McMahon et al. 2013, Troina et al. 2020a). In the southern area, higher $\delta^{15}N$ values result from inputs of ^{15}N-enriched nitrogen sources (e.g. NO_3^-) derived from freshwater discharge (e.g. Río de La Plata) and/or the cold, nutrient-rich subantarctic waters of the Malvinas Current (Garcia 1997, Matsuura & Andrade 2000, McMahon et al. 2013, Troina et al. 2020a). These nutrient-rich waters sustain large biomasses of forage fish like the Argentinean anchovy *Engraulis anchoita* (Madureira et al. 2009, Costa et al. 2016) and lanternfish *Maurolicus stehmanni* (Madureira et al. 2005). These species are key components of the pelagic nektonic food webs in the SWAO (Velasco & Castello 2005, Gasalla et al. 2007), providing the forage base for several predators such as seabirds (Bugoni et al. 2010, Marques et al. 2018, Costa et al. 2020a), marine mammals (Troina et al. 2020b), and large pelagic fish including tunas (Castello et al. 1997).

Previous work on skipjack feeding habits in the SWAO indicated that lanternfish, euphausiids (*Euphausia similis*), and anchovy are the key food items for the species (Ankenbrandt 1985, Vilela 1990, Coletto et al. 2020). Mixing models combining $\delta^{15}N$ and carbon isotope ($\delta^{13}C$) data with informative priors derived from SCA found that lanternfish, krill (*E. similis*), and small pelagic fish (i.e. anchovies and sardines) were the primary food sources in this region (Coletto et al. 2021). In general, both SCA and isotope-based estimates of diet composition indi-

cated a decrease in the importance of euphausiids and an increase in the proportion of fish with increasing skipjack size (Ankenbrandt 1985, Coletto et al. 2020, 2021). These results indicate that skipjack may increase its TP over ontogeny, however, spatial and size-related shifts in skipjack TP in the SWAO have not been examined to date.

Additionally, our previous work with bulk tissue SIA in the SWAO indicated that $\delta^{15}N$ values of skipjack and euphausiids (Coletto et al. 2021) mirrored those of zooplankton $\delta^{15}N$ isoscapes (Troina et al. 2020a). This result suggests that schools have a degree of residency at the timescale of isotopic turnover for muscle in the SWAO feeding grounds, and that spatial patterns in the baseline isotopic composition could be exploited to characterize seasonal movements of marine consumers in this region (Coletto et al. 2021). Because $\delta^{15}N_{bulk}$ values decrease with skipjack size in the SWAO, and there is an increase in the consumption of larger prey with increasing skipjack size, we speculate that rather than feeding at a lower trophic level, adults may forage in areas characterized by lower $\delta^{15}N$ baselines (Troina et al. 2020a). Therefore, we aimed to use AA $\delta^{15}N$ analysis as an additional proxy to support bulk tissue isotope-based inferences of skipjack foraging habitat in the SWAO.

Here, we used a multi-proxy approach to study ontogenetic patterns in skipjack foraging habitat and TP in the SWAO. Specifically, we used (1) AA $\delta^{15}N$ analysis to explore ontogenetic shifts in skipjack foraging habitat to test if the decrease in $\delta^{15}N_{bulk}$ found by Coletto et al. (2021) in large-sized individuals is related to foraging in areas with lower $\delta^{15}N$ baselines; and (2) SCA along with bulk tissue and AA $\delta^{15}N$ analysis to characterize spatial and ontogenetic variation in skipjack TP. The AA $\delta^{15}N$ analysis allowed us to separate the effects of foraging across multiple habitats with distinct $\delta^{15}N$ baselines from changes in skipjack TP with ontogeny. In addition, our results have methodological implications for how AA $\delta^{15}N$ data are used to evaluate spatial variation in baseline $\delta^{15}N$ values and TP in top marine consumers.

2. MATERIALS AND METHODS

2.1. Sampling

Samples used in this study were collected from fishing fleet landings between December 2016 and May 2018 at Niterói and Rio Grande, Brazil (Fig. 1). Further details on each data set used are given in the following sections. Catch positions were obtained from logbooks and plotted using QGIS software (version 3.4.9). Samples were classified by depth strata using QGIS as follows: inner shelf (depth: <100 m),

Fig. 1. Distribution of skipjack tuna samples collected in the southwestern Atlantic Ocean. Symbols in the northern (red) and southern (green) areas indicate techniques used to estimate trophic position: stomach content analysis (SCA, triangles); bulk tissue $\delta^{15}N$ analysis (bulk-$\delta^{15}N$, medium circles); and amino acid nitrogen analysis (AA-$\delta^{15}N$, large circles). Isobaths are shown in gray scale with increasing depth. Inset shows the Subtropical Convergence Area and major currents in the region: North Brazil Current (NBC), Brazil Current (BC), Malvinas Current (MC)
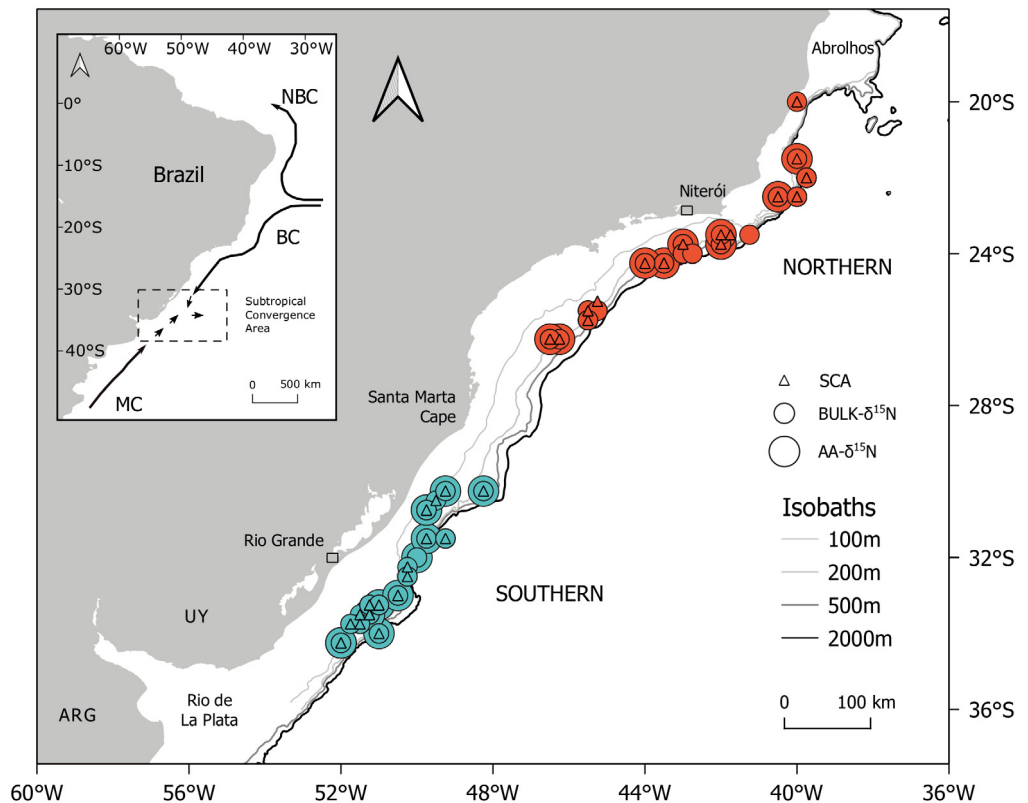
outer shelf (100–200 m), shelf break and slope (200–500 m), and offshore (>500 m). Specimens were weighed (g) and measured for straight fork length (SFL) to the nearest centimeter. The overall range of SFL for skipjack included in SCA was 36.5–83.0 cm (n = 740), 37.0–80.0 cm for $\delta^{15}N_{bulk}$ analysis (n = 383), and 39.0–80.0 cm for AA $\delta^{15}N$ analysis (n = 38). Sample sizes were consistent across areas and size classes except for adults in the southern area, which had a small sample size because adults are less abundant in this area (Table 1). Size groups were defined according to the SFL at first maturity (L_{50} = 46 cm), and the SFL at which all individuals are mature (L_{100} = 63 cm) in the SWAO (Benevenuti Soares et al. 2019). Size groups were defined as juvenile (SFL: <47 cm), young adult (47–63 cm), and adult (> 64 cm).

2.2. AA $\delta^{15}N$ analysis

For AA $\delta^{15}N$ analysis, skipjack white muscle samples (n = 38) collected between January 2017 and February 2018 were selected from the bulk tissue data set published in Coletto et al. (2021). Samples were selected according to location of capture (northern and southern areas) and SFL to maximize analysis across ontogeny. Due to the low C:N ratios (3.2 ± 0.1) observed in the bulk tissue data set, we did not extract lipids from muscle tissues prior to AA $\delta^{15}N$ analysis (Post et al. 2007). Approximately 10 mg of muscle tissue was hydrolyzed to its constituent AAs in 1 ml of 6 N HCl at 110°C for 20 h; tubes were flushed with N_2 and tightly sealed to prevent oxidation during hydrolysis. Acid hydrolysis converts glutamine into glutamic acid (hereafter denoted as Glx) and asparagine to aspartic acid. AAs were then derivatized to *N*-trifluoro-

acetic acid isopropyl esters following established protocols (Silfer et al. 1991, Whiteman et al. 2019). Samples were derivatized in batches alongside in-house AA reference material containing a mixture of 13 AAs of known isotopic composition. Samples were injected by a Thermo Scientific TriPlus RSH Autosampler into a Thermo Scientific Trace 1310 Gas Chromatograph (GC) outfitted with a 60 m × 0.32 mm ID BPX5 × 1.0 µm GC column (inlet temperature: 250°C). The GC oven ramped from 70 to 300°C (70°C hold for 1 min, increase to 120°C at a rate of 15°C min^{-1}, increase to 195°C at 4°C min^{-1}, increase to 235°C at 5°C min^{-1}, increase to 300°C at 15°C min^{-1}, hold at 300°C for 8 min) and separated, gaseous-derivatized AAs were reduced into N_2 at 1000°C in a Thermo Scientific IsoLink II combustion reactor. The N_2 gas was sent to a Thermo Scientific Delta V Plus IRMS via a Conflo IV for isotopic analysis at the University of New Mexico Center for Stable Isotopes (Albuquerque, NM). Samples were analyzed in duplicate or triplicate and bracketed by injections of the in-house AA reference material. Analytical precision, measured as the mean within-run standard deviation of Glx, Lys, and Phe, was 0.3‰. All bulk tissue and AA $\delta^{15}N$ data are reported in δ-notation calibrated to the internationally accepted standard of atmospheric N_2 (AIR).

2.3. AA data analyses

Statistical analyses were performed in R v.3.6.0 (R Core Team 2019). Since $\delta^{15}N_{Glx}$ and $\delta^{15}N_{Lys}$ values met normality and homoscedasticity assumptions, Student's *t*-tests were used to compare $\delta^{15}N_{Glx}$ and $\delta^{15}N_{Lys}$ values between the northern and southern areas. $\delta^{15}N_{Phe}$ values were compared between areas with a non-parametric Wilcoxon test, because the data were not normally distributed and homoscedastic. Pairwise Wilcoxon tests with Bonferroni-adjusted p-values for multiple comparisons were used to compare $\delta^{15}N_{Glx}$, $\delta^{15}N_{Lys}$, and $\delta^{15}N_{Phe}$ values among size classes (juvenile, young adult, adult) within areas. We plotted $\delta^{15}N_{Glx}$ vs. $\delta^{15}N_{Lys}$ values and $\delta^{15}N_{Glx}$ vs. $\delta^{15}N_{Phe}$ values to identify patterns between areas and size classes in AA $\delta^{15}N$ values for skipjack and to identify individuals that had $\delta^{15}N$ values distinct from their area of sampling.

Skipjack $\delta^{15}N_{bulk}$ values varied with latitude of collection (Coletto et. al

Table 1. Sample size (n) and mean ± SD straight fork length (SFL, cm) for sampled skipjack used to estimate trophic position via stomach content analysis (TP_{SCA}), bulk tissue $\delta^{15}N$ (TP_{bulk}), and amino acid (TP_{AA}) $\delta^{15}N$ analysis grouped by size class and area of capture in the southwestern Atlantic Ocean

Area	Size class	TP_{SCA}		TP_{bulk}		TP_{AA}	
		n	SFL	n	SFL	n	SFL
Northern		355	53.0 ± 10.2	242	51.3 ± 9.3	18	58.2 ± 14.2
	Juvenile	112	42.8 ± 2.8	78	41.8 ± 2.1	5	40.9 ± 3.0
	Young adult	187	53.7 ± 4.6	130	52.5 ± 4.6	5	53.7 ± 5.3
	Adult	56	71.2 ± 5.5	34	68.4 ± 4.6	8	71.8 ± 5.3
Southern		385	51.2 ± 5.5	141	52.3 ± 6.4	20	49.9 ± 5.7
	Juvenile	99	45.0 ± 1.9	26	43.9 ± 2.3	7	44.7 ± 1.7
	Young adult	278	53.0 ± 4.0	108	53.4 ± 4.4	12	51.7 ± 3.9
	Adult	8	66.4 ± 3.4	7	66.3 ± 3.9	1	64.0
	Total	740		383		38	

2021) in agreement with zooplankton $\delta^{15}N$ isoscapes in the SWAO (Troina et al. 2020a). To evaluate which source AA best reflects patterns in skipjack $\delta^{15}N_{bulk}$, we used linear models of $\delta^{15}N_{bulk}$ values vs. $\delta^{15}N_{Lys}$ and $\delta^{15}N_{Phe}$ values, using the coefficient of determination (R^2) to assess the goodness of fit.

2.4. Baseline mixing model

To determine the relative contribution of the northern and southern areas for skipjack size classes, we used a 2 end-member mixing model in the stable isotope mixing models package in R ('simmr'; Parnell 2019). We used $\delta^{15}N$ of Lys and Phe for juveniles as end-members for each area in the mixing model: northern $\delta^{15}N_{Lys} = 3.5 \pm 0.1$‰ (n = 3) and southern $\delta^{15}N_{Lys} = 6.1 \pm 0.8$‰ (n = 6); northern $\delta^{15}N_{Phe} = 7.8 \pm 1.4$‰ (n = 3) and southern $\delta^{15}N_{Phe} = 10.5 \pm 0.8$‰ (n = 6). Juveniles with $\delta^{15}N$ values that differed from the area of sampling were considered recent migrants. These were not used to calculate end-member baseline values. See further details below and in Table S1 in the Supplement at www.int-res.com/articles/suppl/m690p147_supp.pdf for measured isotope values. This approach assumes that skipjack spend at least 3–4 mo in the northern or southern areas of the SWAO (Coletto et al. 2021), which is similar in duration to half-lives estimated for nitrogen isotopes in the bulk (white) muscle tissue (5.5 mo; Madigan et al. 2012) and muscle Lys (4.5 mo; Bradley et al. 2014) in bluefin tuna. Isotopic incorporation rates are likely faster in skipjack relative to bluefin tuna, because skipjack have the highest growth rates among tuna species (Murua et al. 2017). Results are reported as the median and 95% credibility intervals for the proportion of each baseline reflected in skipjack size classes. We estimated the contribution of the 2 isotopic baselines (northern and southern) to skipjack of each size class. This result is reported as the probability of one baseline proportion being higher than the other, which is obtained using the function 'compare_sources' in 'simmr'.

To identify recent migrants that had anomalous (outlier) $\delta^{15}N_{Lys}$ values within areas, we used a 2-end-member mixing model as follows: $\alpha = (\delta^{15}N_{Lys-cons} - \delta^{15}N_{Lys-South}) / (\delta^{15}N_{Lys-North} - \delta^{15}N_{Lys-South})$, where α is the proportion of the northern baseline in consumer tissue, $\delta^{15}N_{Lys-cons}$ are the measured $\delta^{15}N_{Lys}$ values of each sample, and $\delta^{15}N_{Lys-North}$ and $\delta^{15}N_{Lys-South}$ are the baseline end-members for the northern and southern areas, as indicated above, respectively. Individuals that had a proportion greater than 75% of a baseline

other than the regional baseline from which they were captured were considered recent migrants.

2.5. TP via AA $\delta^{15}N$ analysis

The AA $\delta^{15}N$-based TP estimates for skipjack (n = 38) were calculated using the equation $TP_{Tr-Sr} = [(\delta^{15}N_{Tr} - \delta^{15}N_{Sr} - \beta) / TDF_{AA}] + 1$, where $\delta^{15}N_{Tr}$ and $\delta^{15}N_{Sr}$ are the $\delta^{15}N$ values for trophic and source AAs, β is the difference between the $\delta^{15}N$ values of the selected trophic and source AAs in primary producers, and TDF_{AA} is the trophic discrimination factor representing the increase in $\delta^{15}N$ values of the trophic relative to the source AA per trophic level. We calculated 2 TP estimates using a combination of 2 trophic–source AAs: one using Glx-Lys $\delta^{15}N$ values ($TP_{Glx-Lys}$) and one using Glx-Phe $\delta^{15}N$ values ($TP_{Glx-Phe}$). We used mean ($\pm SD$) $\beta_{Glx-Lys}$ (3.9 $\pm$ 0.5‰), $\beta_{Glx-Phe}$ (3.6 $\pm$ 0.5‰), $TDF_{Glx-Lys}$ (5.2 $\pm$ 0.3‰), and $TDF_{Glx-Phe}$ (5.7 $\pm$ 0.3‰) values derived from a meta-analysis of marine teleosts (Bradley et al. 2015). We also calculated TP using TDFs reported by Bradley et al. (2014) ($TDF_{Glx-Lys} = 8.1 \pm 0.4$‰; $TDF_{Glx-Phe} = 6.3 \pm 0.4$‰) as well as Nuche-Pascual et al. (2021) ($TDF_{Glx-Lys} = 6.2 \pm 2.2$‰; $TDF_{Glx-Phe}$ 6.2 $\pm$ 2.1‰). Finally, we calculated TP using the weighted mean $\delta^{15}N$ values of trophic (alanine, leucine, Glx) and source (Phe, Lys, glycine) AAs (TP_{Tr-Sr}; Choy et al. 2015). We used the mean ($\pm SD$) for β_{Tr-Sr} (3.6 $\pm$ 0.5‰) and TDF_{Tr-Sr} (5.7 $\pm$ 0.3‰). Errors were propagated following equations available in Dale et al. (2011) and Sabadel et al. (2020) by combining the analytical uncertainty in AA $\delta^{15}N$ values with the uncertainty in β_{Tr-Sr} and TDF_{Tr-Sr}. $TP_{Glx-Lys}$, $TP_{Glx-Phe}$, and TP_{Tr-Sr} were compared between areas (northern vs. southern) using Student's t-tests. Pairwise Wilcoxon tests with Bonferroni-adjusted p-values for multiple comparisons were used to compare $TP_{Glx-Lys}$, $TP_{Glx-Phe}$, and TP_{Tr-Sr} among size classes (juvenile, young adult, adult) within areas.

2.6. TP via SCA

We used a data set (n = 740) of samples collected during 2016–2018 (Coletto et al. 2020) for calculating TP based on SCA (TP_{SCA}). Stomach contents were removed and kept frozen or fixed in formalin (10%) until further processing in the laboratory. Food items were sorted and identified to the lowest taxon possible using identification keys for Crustacea, Mollusca, and Teleostei (e.g. Figueiredo & Menezes 1980, Gibbons et al. 1999, Haimovici et al. 2009). For each indi-

vidual stomach, prey items from each category were weighed (g) and counted. The degrees of digestion were determined using criteria developed by Vaske et al. (2004). Bait species (i.e. *Sardinella brasiliensis, Engraulis anchoita*) found in skipjack stomachs in the initial stages of digestion (i.e. non-digested, starting digestion) were removed from the analysis, assuming they were not ingested as natural food.

TP_{SCA} was calculated as $TP_{SCA} = 1 + (\sum_1^n P_i \times TP_i)$, where n is the number of prey categories, P_i is the mass proportion of prey category *i*, and TP_i is the TP of prey category *i* (Cortés 1999). In total, 12 prey categories belonging to 3 taxonomic groups (i.e. Crustacea, Mollusca, Teleostei) were used to calculate TP_{SCA} for skipjack. TPs of prey categories reported in the literature and their mass percentages are provided in Table S2. TP for the unidentified Teleostei was calculated through the weighted mean of mass of fish prey categories. An average TP of 2.4 from 2 independent estimates was used as euphausiids': *Euphausia pacifica* (TP = 2.5; Sogawa et al. 2017) and *Thysanopoda* spp. (TP = 2.3; Hannides et al. 2009).

2.7. TP via $\delta^{15}N_{bulk}$ analysis

We estimated bulk tissue TP (TP_{bulk}) with $\delta^{15}N$ data for 383 skipjack collected between 2016–2018 and published in Coletto et al. (2021). Further information on the collection, storage, and treatment of muscle samples prior to isotope analysis can be found in Coletto et al. (2021). The Bayesian package 'tRophicPosition' (Quezada-Romegialli et al. 2019) in R (R Core Team 2019) was used to estimate TP_{bulk} by area (northern and southern) and size class (juvenile, young adult, adult) within each area. This approach includes sources of variation for $\delta^{15}N$ baseline estimates and consumer-diet TDFs to provide robust estimates of TP. We used the 'Onebaseline' model to account for the difference in $\delta^{15}N$ values in primary consumers and skipjack bulk tissue between areas in the SWAO (Troina et al. 2020a, Coletto et al. 2021). The 'Onebaseline' model assumes that a consumer's $\delta^{15}N$ value is equal to $\delta^{15}N_{baseline} + TDF(TP - \lambda)$; where $\delta^{15}N_{baseline}$ is the isotopic signature of the baseline organism, TDF is the trophic discrimination factor for each step in the food web, and λ is the TP of the baseline organism (Quezada-Romegialli et al. 2019), which is represented by zooplankton in our models. Published $\delta^{15}N$ values for copepods sampled along the shelf break in the SWAO were used as proxies for the isotopic baseline in each area (northern: $\delta^{15}N_{copepods} = 4.3 \pm 1.7‰$, n = 12; southern:

$\delta^{15}N_{copepods} = 6.1 \pm 2.3‰$, n = 21; Troina et al. 2020a). Because the majority of adult skipjack (62%) sampled in the northern area were caught in offshore waters (i.e. depth >500 m; Figs. S1 & S2), we used the mean $\delta^{15}N$ value for copepods collected from shelf break and offshore waters ($\delta^{15}N_{copepods} = 2.8 \pm 1.3‰$, n = 28; Troina et al. 2020a) as an isotopic baseline to estimate adult TPs in this area. The baseline TP for copepods was set to 2.2 assuming a low degree of omnivory (i.e. 80% grazing, 20% predation), which is in the lower range of TP estimates for copepod species in the North Pacific (Hannides et al. 2009). Studies show that TDFs for $\delta^{15}N$ can vary with form of nitrogen excretion, tissue type, environment, taxa, and diet quality (Post 2002, McCutchan et al. 2003, Vanderklift & Ponsard 2003, Caut et al. 2009). We selected published TDF values for muscle of marine ammoniotelic fish ($\Delta^{15}N$: 3.7‰) and calculated the uncertainty around the mean value by subtracting the maximum from the minimum estimate divided by 2 (Table S3). We also estimated TP_{bulk} using the mean TDF for marine fishes based on the meta-analysis reported in Vanderklift & Ponsard (2003) ($\Delta^{15}N$: 2.4‰). The function 'simulateTDF' was used to include TDF values and their variability in the models. Simulations were run with 4 chains and 20 000 adaptations.

3. RESULTS

3.1. Glx, Lys, and Phe $\delta^{15}N$ values

Skipjack collected in the southern area had higher $\delta^{15}N_{Glx}$ ($t = -3.16$, df = 32.4, p < 0.05), $\delta^{15}N_{Lys}$ ($t = -4.48$, df = 31.7, p < 0.001), and $\delta^{15}N_{Phe}$ (Wilcoxon test, $W = 80$, p < 0.05) values than in the northern area (Table 2). There was a significant positive correlation between skipjack muscle $\delta^{15}N_{Glx}$ and $\delta^{15}N_{Lys}$ values (Fig. 2A): $\delta^{15}N_{Glx} = 0.56 (\pm 0.1) \times \delta^{15}N_{Lys} - 20.11 (\pm 0.5)$; ($F_{1,36} = 32.59$, p < 0.001, $R^2 = 0.46$) as well as between $\delta^{15}N_{Glx}$ and $\delta^{15}N_{Phe}$ values (Fig. 2B): $\delta^{15}N_{Glx} = 0.40 (\pm 0.1) \times \delta^{15}N_{Phe} - 19.13 (\pm 1.3)$; ($F_{1,36} = 9.68$, p < 0.05, $R^2 = 0.19$). There was a stronger relationship between $\delta^{15}N_{bulk}$ and $\delta^{15}N_{Lys}$ values (Fig. 3A; $F_{1,36} = 174.2$, p < 0.001, $R^2 = 0.82$) in comparison to $\delta^{15}N_{bulk}$ and $\delta^{15}N_{Phe}$ values (Fig. 3B; $F_{1,36} = 17.4$, p < 0.001, $R^2 = 0.30$). $\delta^{15}N_{Glx}$, $\delta^{15}N_{Lys}$, and $\delta^{15}N_{Phe}$ values did not differ among size groups in either area (pairwise Wilcoxon test, p > 0.05) (Table 2). In the southern area, $\delta^{15}N_{Lys}$ values increased sharply with skipjack size up to ~54 cm SFL and then decreased in skipjack larger than ~55 cm

Table 2. Mean (±SD) and range of $\delta^{15}N$ values for glutamic acid (Glx), lysine (Lys), and phenylalanine (Phe) of skipjack size classes for each area of the southwestern Atlantic Ocean. Corrected (corr) mean $\delta^{15}N$ values used in mixing models do not include outliers (n = 6) that had $\delta^{15}N$ values indicative of recent migration from another area

| Area	Size class	n	$\delta^{15}N_{Glx}$ (‰)	$\delta^{15}N_{Glx\ corr}$ (‰)	$\delta^{15}N_{Lys}$ (‰)	$\delta^{15}N_{Lys\ corr}$ (‰)	$\delta^{15}N_{Phe}$ (‰)	$\delta^{15}N_{Phe\ corr}$ (‰)
Northern		19	22.3 ± 1.6 (20.1–25.7)	21.8 ± 1.1	4.1 ± 1.8 (1.6–8.2)	3.4 ± 1.1	8.9 ± 1.9 (6.7–12.8)	8.2 ± 1.2
	Juvenile	5	22.0 ± 2.3 (20.1–25.6)	20.6 ± 0.6	5.1 ± 2.3 (3.4–8.2)	3.5 ± 0.1	9.7 ± 2.9 (6.7–12.8)	7.8 ± 1.4
	Young adult	5	22.8 ± 1.8 (20.9–25.7)	22.1 ± 0.9	4.6 ± 1.3 (3.2–6.3)	4.2 ± 1.0	8.7 ± 1.8 (6.9–11.3)	8.0 ± 1.3
	Adult	8	22.2 ± 1.0 (20.9–23.5)	22.2 ± 1.0	3.0 ± 1.2 (1.6–5.0)	3.0 ± 1.2	8.5 ± 1.2 (7.3–11.2)	8.5 ± 1.2
Southern		20	23.8 ± 1.2 (20.8–25.6)	23.9 ± 1.2	6.3 ± 1.3 (3.9–8.4)	6.5 ± 1.3	10.6 ± 1.3 (8.6–13.0)	10.6 ± 1.3
	Juvenile	7	23.2 ± 1.7 (20.8–25.6)	23.5 ± 1.7	5.8 ± 1.1 (4.1–7.3)	6.1 ± 0.8	10.3 ± 0.8 (9.1–11.2)	10.5 ± 0.8
	Young adult	12	24.1 ± 0.9 (22.5–23.6)	24.1 ± 0.9	6.9 ± 1.2 (4.5–8.4)	6.9 ± 1.2	10.6 ± 1.5 (8.6–13.0)	10.6 ± 1.5
	Adult	1	23.6	23.6	3.9	3.9	11.4	11.4
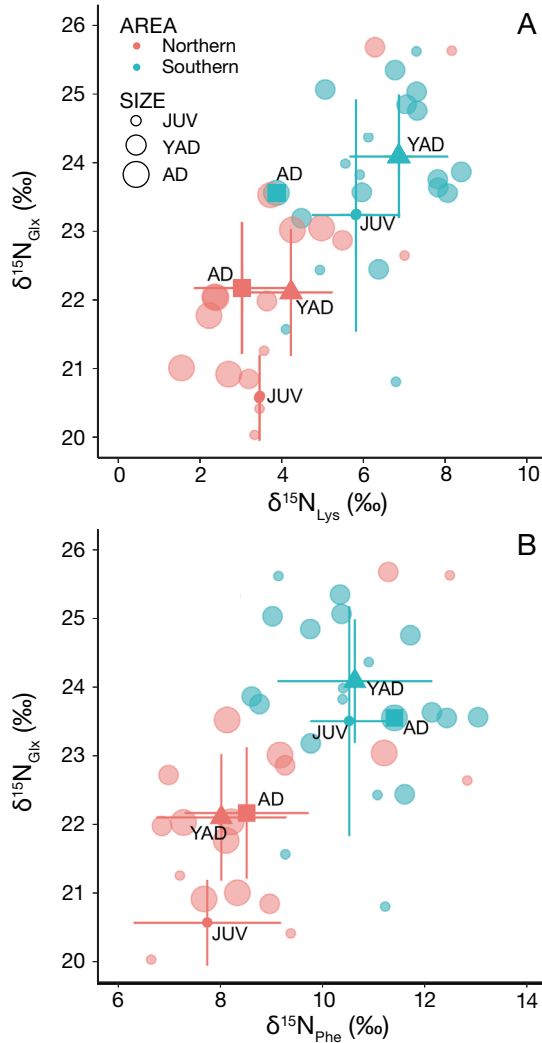
Fig. 2. Relationship between $\delta^{15}N$ values for (A) glutamic acid (Glx) (trophic amino acid [AA]) and lysine (Lys) (source AA), and (B) Glx and phenylalanine (Phe) (source AA). Circle size denotes size class; symbols represent mean values for size classes for each area: juvenile (JUV, circle), young adult (YAD, triangle), adult (AD, square). Error bars: ±1 SD
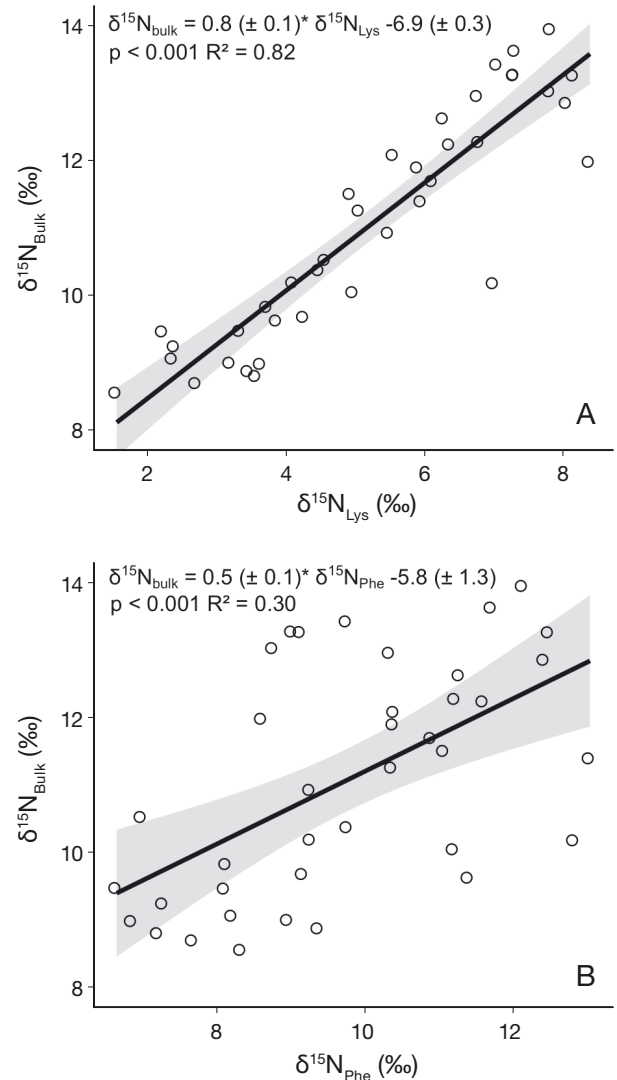

Fig. 3. Relationship between (A) $\delta^{15}N_{bulk}$ and $\delta^{15}N_{Lys}$ values and (B) $\delta^{15}N_{bulk}$ and $\delta^{15}N_{Phe}$ values for skipjack in the southwestern Atlantic Ocean. Shaded areas: 95% confidence interval for each model slope

SFL (Fig. 4A). A similar pattern was observed in skipjack collected from the northern area. $\delta^{15}N_{Phe}$ values also increased with skipjack size up to ~60 cm SFL in both areas and decreased in large skipjack in the northern area (Fig. 4B).

3.2. Baseline mixing model

The relative contribution of the northern and southern areas reflected in $\delta^{15}N_{Lys}$ and $\delta^{15}N_{Phe}$ values assumed to represent the baseline differed among size classes (Fig. 5). The mixing model with $\delta^{15}N_{Lys}$ values indicated a higher proportion of the southern baseline in juveniles (73%) and young adults (88%) relative to the northern area (probabilities = 0.9 and 1.0, respectively). Adults had a higher proportion of the northern baseline (89%) relative to the southern baseline (probability = 1.0). Similarly, the mixing model with $\delta^{15}N_{Phe}$ values indicated a higher proportion of the southern baseline in juveniles (75%) and young adults (78%) (probabilities = 0.9 and 1.0, respectively) in comparison to adults, which had a higher contribution of the northern baseline (62%) relative to the southern baseline (probability = 0.7). Mixing models using $\delta^{15}N_{Lys}$ values to quantify the relative proportion of baselines between areas for individual skipjack showed that 4 individuals caught in the northern area had high $\delta^{15}N_{Lys}$ values, indicating that they had recently moved from the southern area (Fig. 6). Likewise, 2 individuals sampled in the southern area had $\delta^{15}N_{Lys}$ values indicative of recent migration from the northern area (Fig. 6).

Fig. 4. Relationship between skipjack straight fork length and $\delta^{15}N$ values for the source amino acids (A) lysine ($\delta^{15}N_{Lys}$) and (B) phenylalanine ($\delta^{15}N_{Phe}$) in the southwestern Atlantic Ocean
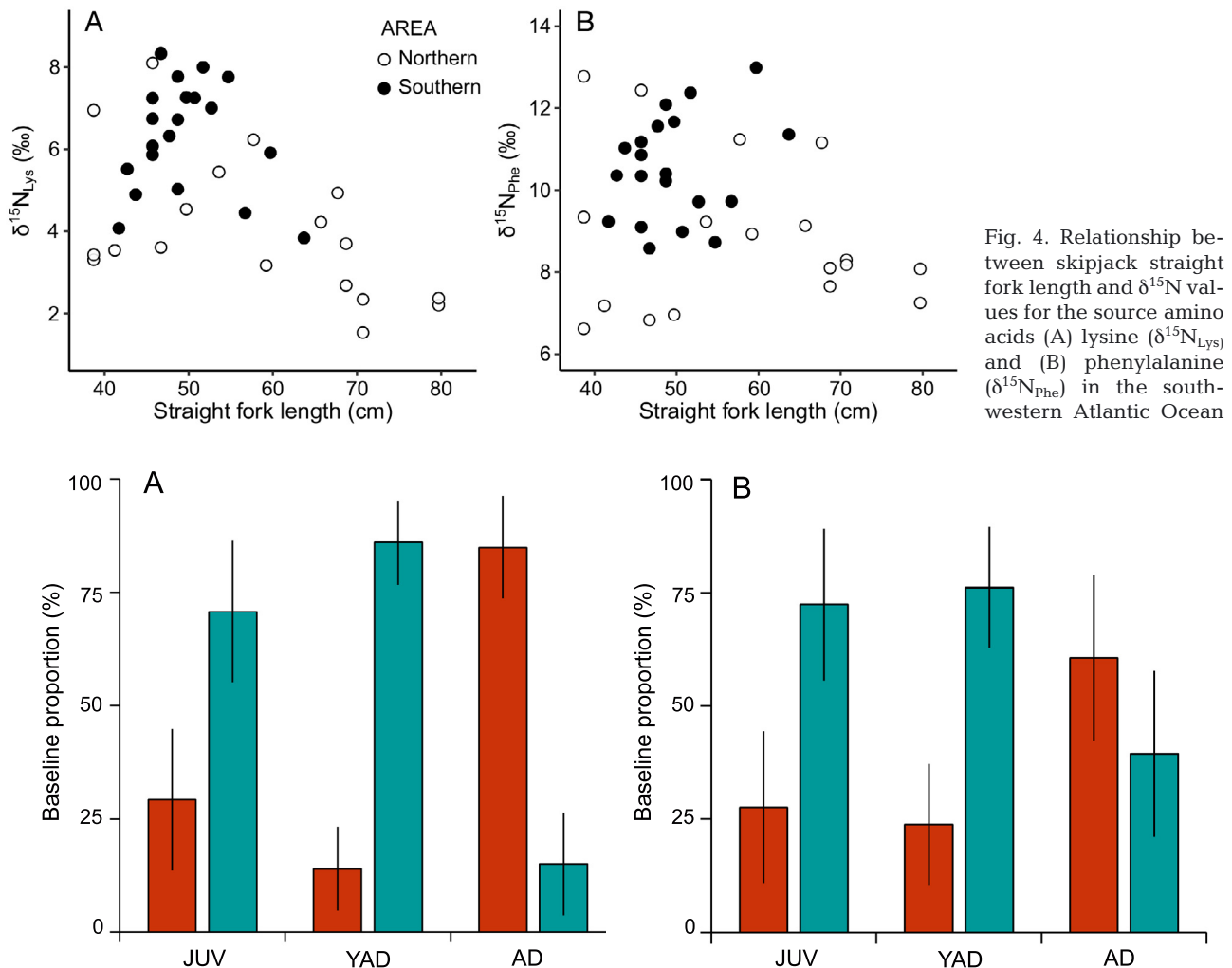
Fig. 5. Estimated mean (±SD) contribution of the northern (red) and southern (green) regional nitrogen isotopic baselines to skipjack muscle tissue in the southwestern Atlantic Ocean, inferred from source amino acids (A) lysine and (B) phenylalanine. JUV: juvenile; YAD: young adult; AD: adult
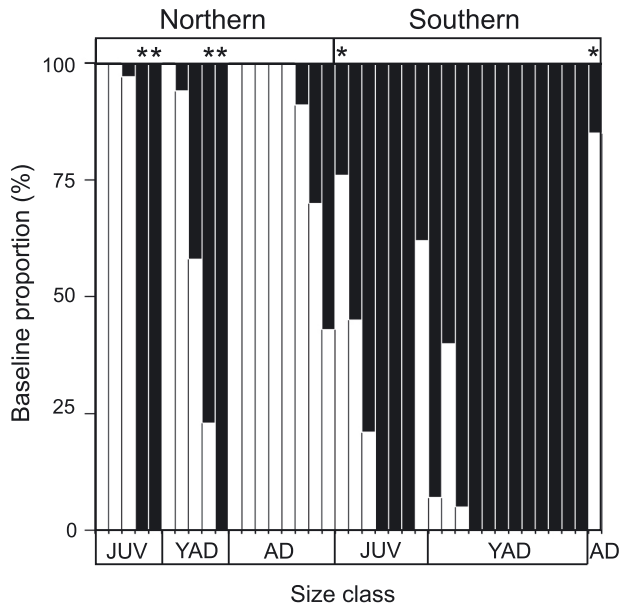
Fig. 6. Relative contribution of the northern (white) and southern (black) regional $\delta^{15}N_{Lys}$ baselines to individual skipjack tissue (n = 38). Asterisks indicate individuals that had a proportion greater than 75% of a baseline other than the regional baseline from which they were captured. Area of sample collection is indicated at the top; size class is indicated at the bottom (JUV: juvenile; YAD: young adult; AD: adult)

3.3. Diet composition

Prey identified from skipjack stomach contents were separated into 12 categories (Table S2). In the northern area, Teleostei was the most important taxonomic group (91% mass [%M]) (Table S2). Among fish prey families, Clupeidae had the highest mass percentage (46%M), followed by unidentified fish (33%M), and Carangidae (10%M). Crustaceans (euphausiids) were of minor importance in the northern area (8%M). With increasing skipjack size, the importance of euphausiids (juvenile: 14%M; young adult: 13%M; adult: 0%M) and Clupeidae (juvenile: 55%M; young adult: 49%M; adult: 38%M) declined. The importance of Carangidae (juvenile: 0%M; young adult: 3%M; adult: 20%M) and unidentified fish (juvenile: 22%M; young adult: 28%M; adult: 42%M) increased with skipjack size (Table S2).

In the southern area, Crustacea (euphausiids) was the most important prey for skipjack (71%M), followed by Teleostei (26%M) represented by unidentified fish (12%M), Sternoptychi-

dae (lanternfish; 7%M), and Engraulidae (6% M). With increasing skipjack size, the importance of euphausiids (juvenile: 75%M; young adult: 71%M; adult: 59%M) declined. There were small shifts in the importance of Engraulidae (juvenile: 6%M; young adult: 6%M; adult: 0%M). The importance of Sternoptychidae (juvenile: 5%M; young adult: 7%M; adult: 0%M) increased from juveniles to young adults (Table S2). Overall, Mollusca had a small contribution to skipjack stomach contents by mass in both the northern (1%M) and southern areas (2%M), except for adults, which consumed Argonautidae (24%M) and unidentified gastropods (16%M) in the southern area.

3.4. TP_{SCA}, TP_{bulk}, $TP_{Glx-Lys}$, $TP_{Glx-Phe}$, and TP_{Tr-Sr}

Mean (±SD) TP_{SCA} for all skipjack in the SWAO was 3.7 ± 0.2. TP_{SCA} was slightly but not significantly higher for skipjack caught in the northern (3.8) than the southern area (3.6) (Table 3). TP_{SCA} increased slightly with skipjack size in the northern area (3.8–3.9) in comparison to the southern area (3.5–3.9) (Table 3, Fig. 7).

TP_{bulk} was similar between the northern (3.7) and southern (3.8) areas (Table 3). In the northern area, adults had higher TP_{bulk} (4.0) in comparison to young adults (3.8; probability = 0.9) and juveniles (3.5; probability = 1) (Fig. 7). In the southern area, young adults had higher TP_{bulk} (3.9) in comparison to juveniles (3.6; probability = 0.9) (Fig. 7). TP_{bulk} estimates for adults in the southern area were similar to those

Table 3. Trophic position (TP) estimates for skipjack in the southwestern Atlantic Ocean grouped by area of capture, size class, and method of estimation. TP was estimated using stomach content analysis (TP_{SCA}), bulk tissue $\delta^{15}N$ analysis (TP_{bulk}), glutamic acid-lysine $\delta^{15}N$ analysis ($TP_{Glx-Lys}$), glutamic acid-phenylalanine $\delta^{15}N$ analysis ($TP_{Glx-Phe}$), and a weighted trophic AA (alanine, leucine, and glutamic acid) and source AA (phenylalanine, lysine, and glycine) $\delta^{15}N$ analysis (TP_{Tr-Sr}). Estimates for TP_{bulk} are reported as a median with 95% credibility intervals, while estimates for $TP_{Glx-Lys}$, $TP_{Glx-Phe}$, and TP_{Tr-Sr} are reported as mean ± SD. Error estimates are not available for the adult from the southern area due to limited sample size (n = 1)

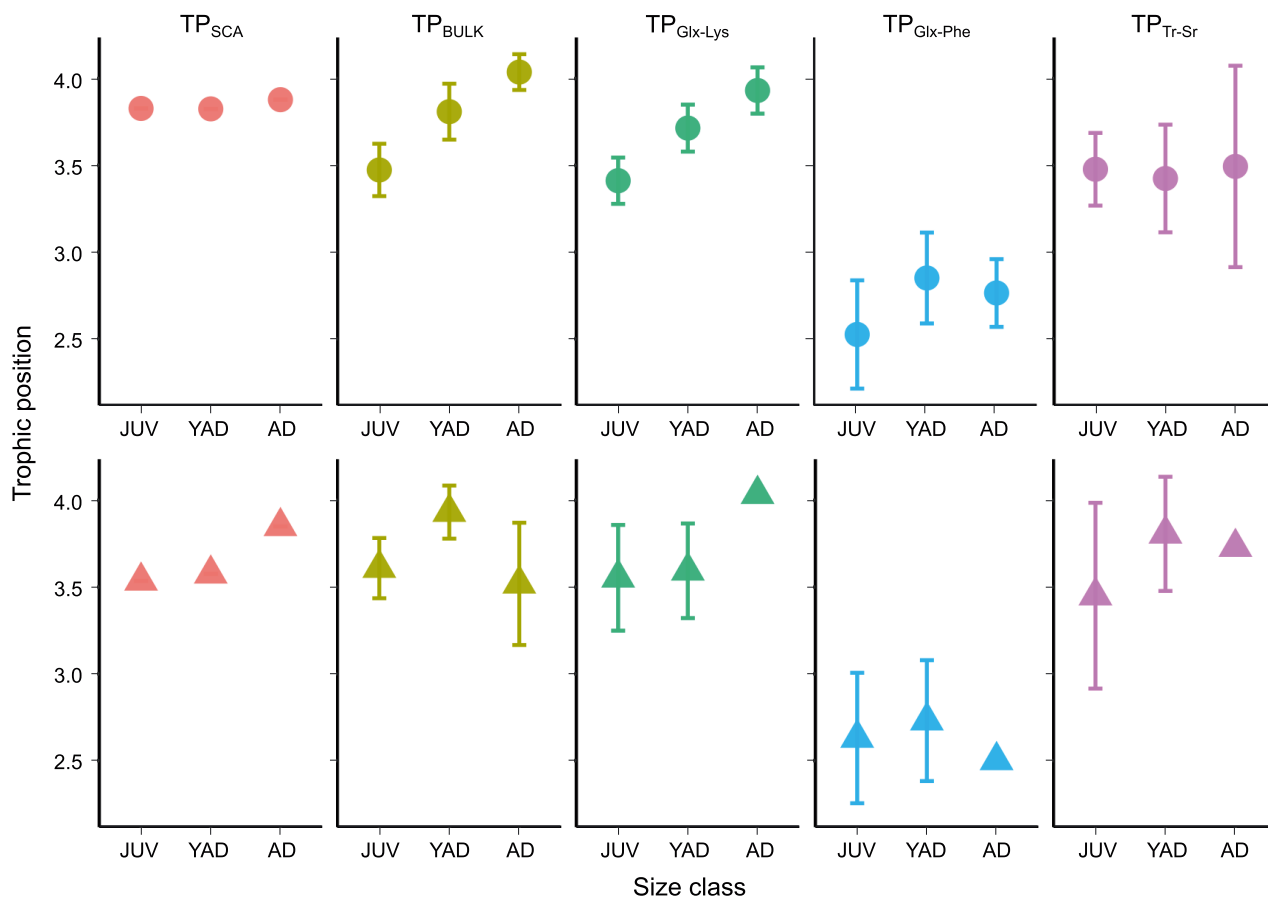| Area	Size class	TP_{SCA}	TP_{bulk}	$TP_{Glx-Lys}$	$TP_{Glx-Phe}$	TP_{Tr-Sr}
North		3.8	3.7 (3.3–4.0)	3.8 ± 0.2	2.7 ± 0.3	3.5 ± 0.4
	Juvenile	3.8	3.5 (3.2–3.8)	3.5 ± 0.2	2.5 ± 0.3	3.5 ± 0.2
	Young Adult	3.8	3.8 (3.5–4.2)	3.7 ± 0.2	2.9 ± 0.3	3.4 ± 0.3
	Adult	3.9	4.0 (3.8–4.2)	3.9 ± 0.1	2.8 ± 0.2	3.5 ± 0.6
South		3.6	3.8 (3.5–4.1)	3.6 ± 0.3	2.7 ± 0.3	3.7 ± 0.4
	Juvenile	3.5	3.6 (3.3–3.9)	3.6 ± 0.3	2.6 ± 0.4	3.5 ± 0.5
	Young Adult	3.6	3.9 (3.6–4.3)	3.6 ± 0.3	2.7 ± 0.3	3.8 ± 0.3
	Adult	3.8	3.5 (2.8–4.2)	4.0	2.5	3.7

Fig. 7. Trophic position (TP) estimates for skipjack in the southwestern Atlantic Ocean by size class (JUV: juvenile; YAD: young adult; AD: adult), area (northern: upper panels; southern: lower panels), and method of estimation. TP was estimated using stomach content analysis (TP$_{SCA}$), bulk tissue δ^{15}N analysis (TP$_{bulk}$), glutamic acid–lysine δ^{15}N analysis (TP$_{Glx-Lys}$), glutamic acid–phenylalanine δ^{15}N analysis (TP$_{Glx-Phe}$), and the difference between weighted average of trophic (alanine, leucine, glutamic acid) and source (phenylalanine, lysine, glycine) amino acids δ^{15}N analysis (TP$_{Tr-Sr}$). Bayesian TP$_{bulk}$ estimates (medians with 95% credibility intervals) are shown in Table 3

of juveniles and were highly variable (Table 3). Values of TP$_{bulk}$ using a TDF of 2.4 were nearly 1 unit higher than those calculated with a TDF of 3.6, following similar patterns when comparing skipjack size classes (Table S4).

TP$_{Glx-Lys}$ varied from 2.9–4.1 with a mean ($\pm$SD) of 3.7 $\pm$ 0.3. The mean TP$_{Glx-Lys}$ for skipjack was similar between the northern (3.8 $\pm$ 0.2) and southern areas (3.6 $\pm$ 0.3) (t = 1.9, df = 35.4, p = 0.06). In the northern area, TP$_{Glx-Lys}$ was higher in adult skipjack (3.9 $\pm$ 0.1) in comparison to juveniles (3.5 $\pm$ 0.2) (pairwise Wilcoxon test, p < 0.05; Fig. 7). TP$_{Glx-Lys}$ were not different among size groups in the southern area (pairwise Wilcoxon test, p > 0.05).

TP$_{Glx-Phe}$ varied from 2.1–3.3 with a mean ($\pm$SD) of 2.7 $\pm$ 0.3, and was similar between the northern (2.7 $\pm$ 0.3) and southern areas (2.7 $\pm$ 0.3) (t = 0.4, df = 35.3, p = 0.7). There were no differences in TP$_{Glx-Phe}$

among size classes in either the northern or southern areas (pairwise Wilcoxon test, p > 0.05; Fig. 7).

TP estimates using alternative TDF values are shown in Table S4. Overall, TP$_{Glx-Lys}$ estimated with TDF$_{Glx-Lys}$ from Nuche Pascual et al. (2021) underestimated TP by approximately one-half a trophic level; TP$_{Glx-Lys}$ estimates based on TDF$_{Glx-Lys}$ from Bradley et al. (2014) and TP$_{Glx-Phe}$ estimates based on TDF from both studies underestimated TP for skipjack by approximately one trophic level in comparison to estimates based on TP$_{SCA}$, TP$_{bulk}$, and TP$_{Glx-Lys}$ (Table S4).

Finally, TP$_{Tr-Sr}$ varied from 2.7–4.7 with a mean ($\pm$SD) of 3.6 $\pm$ 0.4 and was similar between the northern (3.5 $\pm$ 0.4) and southern areas (3.7 $\pm$ 0.4) (t = −1.5, df = 35.7, p = 0.1). There were no differences in TP$_{Tr-Sr}$ among size classes in either the northern or southern areas (pairwise Wilcoxon test, p = 1; Fig. 7).

4. DISCUSSION

We applied multiple techniques to study the foraging habitat and TP of a widely distributed pelagic consumer that plays an important role in food security in the SWAO and worldwide. Our study showed that the SWAO skipjack population uses multiple habitats with distinct $\delta^{15}N$ baselines over its lifetime. Nitrogen isotope values of source AAs Lys and Phe were correlated with $\delta^{15}N_{bulk}$ values, demonstrating that the variation in $\delta^{15}N_{bulk}$ values in skipjack is driven by latitudinal gradients in baseline $\delta^{15}N$ values. Baseline mixing models indicated that the productive southern area (Castello et al. 1997, Matsuura & Andrade 2000) is used by juveniles and young adults, most likely to fuel rapid growth. The decrease in $\delta^{15}N_{Lys}$ and $\delta^{15}N_{Phe}$ values with skipjack size showed that adults forage in warmer oligotrophic areas with lower $\delta^{15}N$ baselines. By disentangling baseline and ontogenetic patterns in $\delta^{15}N$ values with trophic (Glx) and source (Lys) AAs, our results showed that skipjack is a tertiary consumer that increases its TP over ontogeny ($TP_{Glx-Lys}$: 3.5–4.0). Lastly, TP estimates using Phe as the canonical source AA consistently underestimated TP across size classes, while estimates using Lys agreed with those based on SCA and $\delta^{15}N_{bulk}$. Our multi-proxy approach provides novel insights into the foraging habitat, movement dynamics, and TP of skipjack in pelagic food webs of the SWAO, which will better inform ecosystem models and management strategies for the sustainable use of this fishery resource in this region.

4.1. Foraging habitats and movement dynamics

Skipjack captured in the southern area had higher $\delta^{15}N_{Lys}$ and $\delta^{15}N_{Phe}$ values than those captured in the northern area (Table 2). These results were consistent with fine-scale zooplankton (e.g. copepods, euphausiids) $\delta^{15}N$ isoscapes characterized by a positive correlation between baseline $\delta^{15}N$ and latitude and a decrease in baseline $\delta^{15}N$ in offshore waters of the SWAO (Troina et al. 2020a). Bulk tissue and AA $\delta^{15}N$ values in cetaceans foraging along the SWAO showed similar trends mirroring $\delta^{15}N$ baselines (Troina et al. 2020b, 2021). Coletto et al. (2021) reported a trend of increasing skipjack bulk muscle tissue $\delta^{15}N$ values with increasing latitude. Based on our results using Lys and Phe $\delta^{15}N$ values, there is strong evidence indicating that this result was driven by spatial variation in baseline $\delta^{15}N$ values rather than spatial variation in skipjack TP. The relationships between $\delta^{15}N_{bulk}$ and $\delta^{15}N_{Lys}$ ($R^2 = 0.82$) or $\delta^{15}N_{Phe}$ ($R^2 = 0.30$) values confirmed that most of the variation in skipjack $\delta^{15}N$ values is explained by $\delta^{15}N$ variation at the base of the food web in the SWAO (Fig. 3). The much higher goodness-of-fit between $\delta^{15}N_{bulk}$ and $\delta^{15}N_{Lys}$ than $\delta^{15}N_{bulk}$ and $\delta^{15}N_{Phe}$ indicates that Lys may be a more reliable proxy for baseline $\delta^{15}N$ values for skipjack, as Lys undergoes less isotope fractionation between consumer-diet in tunas in comparison to Phe (Bradley et al. 2014). Alternatively, Bradley et al. (2014) found that Lys had faster turnover rates than glycine and serine. Although data for Phe are not available for a direct comparison, Lys in muscle would reach steady-state with local baselines faster if this source AA had a higher isotopic incorporation rate.

Overall, the baseline $\delta^{15}N$ patterns reported in this study for skipjack are consistent with studies on pelagic predators in other ocean basins. The latitudinal pattern in $\delta^{15}N$ values of yellowfin tuna and swordfish *Xiphias gladius* was explained by spatial variation in $\delta^{15}N$ baselines propagating up the food chain in the western Indian Ocean (Ménard et al. 2007). Off eastern Australia, several top predators had $\delta^{15}N_{bulk}$ values that were consistent with a shift from lower baseline $\delta^{15}N$ values in the oligotrophic Coral Sea to higher values in nutrient-rich waters of the Tasman Sea (Revill et al. 2009). In the eastern tropical Pacific, the large range in yellowfin tuna $\delta^{15}N_{bulk}$ values (11‰) was explained by spatial variation in $\delta^{15}N$ baselines (Lorrain et al. 2015). Similarly, $\delta^{15}N_{bulk}$ values in yellowfin and bigeye *Thunnus obesus* tunas were also related to nutrient dynamics in the western central Pacific Ocean, which induce important variability in the $\delta^{15}N$ values at the base of the food web (Popp et al. 2007, Graham et al. 2010, Olson et al. 2010).

In general, skipjack caught in either the southern or northern areas showed $\delta^{15}N_{Lys}$ and $\delta^{15}N_{Phe}$ values consistent with the foraging ground where they were collected, providing strong evidence for local feeding and indicating most of the samples were in steady-state with the local $\delta^{15}N$ baseline. However, some individuals appeared as outliers (Figs. 2 & 6) and showed a mismatch between their $\delta^{15}N$ values and baseline $\delta^{15}N$ values in their area of capture, which likely reflects recent long-distance movements between these 2 isotopically distinct areas. This interpretation agrees with previous work in which $\delta^{15}N$ analysis of source AAs was used to distinguish recent Pacific bluefin tuna migrants from eastern Pacific Ocean residents (Madigan et al. 2014). Isotopically

distinct ecoregions in the western Pacific Ocean were also used to infer previous foraging areas of Pacific bluefin tuna sampled in the spawning grounds off Taiwan, with 2 outlier individuals being identified as potential transoceanic migrators (Madigan et al. 2016).

In our study, 2 individuals caught in the southern area had $\delta^{15}N_{Lys}$ nearly identical to the northern $\delta^{15}N_{Lys}$ baseline (Figs. 2A & 6). One was an adult captured during summer and the other was a juvenile captured during spring (Table S1). The movement of these individuals was likely driven by sea surface temperature dynamics in the SWAO, in which schools move southwards with seasonal shifts in the BC during spring and summer (Matsuura & Andrade 2000). Four additional individuals captured in the northern area had $\delta^{15}N_{Lys}$ values 2.2–4.1‰ higher than mean $\delta^{15}N_{Lys}$ values for this area (Figs. 2A & 6). Cold waters may act as thermal barriers for skipjack, inducing latitudinal movements to avoid waters with SST lower than 18°C (Kiyofuji et al. 2019). Accordingly, 3 of these individuals were caught during the fall, when skipjack schools foraging in the southern area return to lower latitudes as the cold water of the Malvinas Current advances from the south and the BC retracts northwards (Castello & Habiaga 1989, Andrade 2003, Coletto et al. 2019, 2021). Our AA $\delta^{15}N$ results thus corroborate previous studies that demonstrated skipjack move seasonally following SST dynamics in the SWAO (Castello & Habiaga 1989, Matsuura & Andrade 2000) based on spatio-temporal patterns in catch statistics (e.g. Andrade 2003, Coletto et al. 2019), tagging and recapture (e.g. Luckhurst 2014), and intrinsic isotopic markers in bulk tissues (i.e. $\delta^{15}N_{bulk}$) (Coletto et al. 2021). The fourth individual was caught in late January, indicating that some schools may move toward lower latitudes during the summer to initiate spawning (Jablonski et al. 1984).

Our results also showed a decrease in $\delta^{15}N_{Lys}$ and $\delta^{15}N_{Phe}$ values with increasing skipjack size, indicating that adults forage more often in the northern area, which is characterized by lower baseline $\delta^{15}N$. The spatial distribution of skipjack size classes by depth (Figs. S1 & S2) showed that adults were caught more often in the northern area and further offshore in deeper waters, where zooplankton $\delta^{15}N$ values were lower than in higher latitudes and at the continental shelf break (Troina et al. 2020a). This result could be the product of our sampling design, however, previous studies of this population confirm that adults are more frequently caught in the northern area relative to the southern area (e.g. Ankenbrandt

1985, Andrade & Kinas 2004, Benevenuti Soares et al. 2019, Costa et al. 2020b), indicating some geographical structure in the demography of the skipjack population in the SWAO. The higher contribution of the northern isotopic baseline to adult skipjack $\delta^{15}N$ values appears to be linked to foraging and reproduction in warm and permanently stratified tropical waters found in lower latitudes. Although spawning seems to be opportunistic (Cayré & Farrugio 1986, Castello & Habiaga 1989, Vilela & Castello 1993) and distributed throughout the year in areas with SST higher than 24°C in the western Atlantic, larval density is higher during the summer near the Abrolhos Bank and the North Brazil Current (Fig. 1; Jablonski et al. 1984, Matsuura & Andrade 2000, Katsuragawa et al. 2020), indicating that adults use tropical areas at lower latitudes for reproduction.

In contrast to patterns for adults, mixing models indicated higher contribution of the southern area to juveniles and young adults. Higher feeding frequency, reflected as an overall lower frequency of empty stomachs, has been observed in the southern area for every size class, notably for juveniles (Coletto et al. 2020). Previous work also showed that skipjack have higher growth rates in the southern area relative to fish in the northern area, which supports the idea that this area is the primary foraging ground for juveniles and young adults (Costa et al. 2020b). Finally, the conclusion that younger individuals use subtropical areas for feeding and growth is also supported by the high abundance of forage found in the productive waters of the southern area, such as small pelagic fish like anchovy and lanternfish (Matsuura & Andrade 2000, Madureira et al. 2005, 2009) and krill (i.e. *Euphausia similis*) that collectively form the resource base for skipjack in the SWAO (Ankenbrandt 1985, Vilela 1990, Coletto et al. 2021).

4.2. Skipjack foraging ecology and TP

Our multi-proxy estimates of skipjack TP show this species is a tertiary consumer in the pelagic food webs of the SWAO (overall TP range: 3.5–4.0), which is consistent with previous reports of skipjack TP derived from ecotrophic models in this region (TP = 3.5; Gasalla et al. 2007). In contrast, TP estimates reported here are lower than those based on $\delta^{15}N_{bulk}$ analysis of a limited number of skipjack (n = 3) in the SWAO (TP_{bulk} = 4.2 ± 0.4; Bugoni et al. 2010) and those based on AA $\delta^{15}N$ analysis of skipjack in the North Pacific Subtropical Gyre (TP = 4.2 ± 0.4; Choy et al. 2015).

Considering all size classes, TP_{SCA} was slightly higher in the northern area (3.8) than in the southern area (3.6). Previous studies showed that nearly 75% of stomach contents by volume in the northern area were lanternfish *Maurolicus stehmanni* and other teleosts (Ankenbrandt 1985), indicating that teleosts (TP range 2.8–3.0) are an important resource for skipjack in this area (Coletto et al. 2020). Lanternfish distribution is linked to the limit between the South Atlantic Central Water (SACW) and warm tropical waters (Madureira et al. 2005), indicating spatial overlap between skipjack and lanternfish in shelf break/slope habitats in the SWAO (Monteiro-Neto et al. 2020). Ecotrophic models pointed out lanternfish and anchovy are the main trophic links between basal and upper trophic levels in pelagic food webs in the SWAO (Velasco & Castello 2005, Gasalla et al. 2007). In contrast, lower TP_{SCA} estimates in the southern area are likely associated with heavy foraging activity on dense patches of krill, which occupy a lower TP than lanternfish. Andrade (2003) suggested that peaks of skipjack fishing activity in the southern area might be related to availability of *E. similis*, as krill is more abundant in summer over the shelf (Gorri 1995). This is supported by our observations of dense skipjack feeding aggregations in neritic waters in the southern area, where the main prey found in stomach contents was krill (Coletto et al. 2020, Table S2). High prey abundances and oceanographic features such as thermal and chlorophyll fronts as well as a shallow thermocline during summer may result in higher skipjack abundance (i.e. higher catch per unit of effort) in the southern area (Lima et al. 2000, Andrade 2003, Coletto et al. 2019). Collectively, these patterns suggest a higher vulnerability of the stock to overfishing in the southern area, particularly for young skipjack when non-selective fishing methods (e.g. purse seiners) are deployed.

In general, skipjack TP increased through ontogeny, which is likely driven by smaller sized individuals consuming more krill and larger skipjack consuming more teleosts. This pattern was also noted by Ankenbrandt (1985). Our previously published isotope-based estimates of diet composition indicate a higher importance of krill for juveniles, while higher-TP prey such as small pelagic fish, Carangidae, and Ommastrephidae increased in importance for adults (Coletto et al. 2021). These results agree with ontogenetic patterns in vertical habitat use for skipjack. Smaller sized skipjack are epipelagic and forage above the thermocline, while adults can perform short dives into deeper, colder, and less oxy-

genated waters (Bernal et al. 2017, Monteiro-Neto et al. 2020). Increased diving capability enhances access to larger, deep-dwelling mesopelagic micronekton prey of higher TP (Graham et al. 2007, Houssard et al. 2017). For example, vertical movements of large (adult) skipjack tagged in the SWAO were strongly correlated with lanternfish nictemeral behavior (Madureira et al. 2005, Monteiro-Neto et al. 2020). In the eastern equatorial Pacific, skipjack occupy shallow waters at night and use a bounce diving behavior during the day to forage on prey associated with the deep scattering layer (Schaefer et al. 2009, Schaefer & Fuller 2013). Furthermore, global compilations show that deeper foraging yellowfin, bigeye, and albacore *T. alalunga* tunas have higher TP (Pethybridge et al. 2018). TP patterns may also result from differences in the assemblages of primary producers in highly productive nearshore versus oligotrophic offshore waters. For example, in the eastern tropical Pacific, an inshore–offshore increase in yellowfin TP occurred due to greater food chain length resulting from smaller phytoplankton dominating in oligotrophic waters, while larger primary producers generally dominate nutrient-rich regions (Olson et al. 2010), which may shorten food chains and by extension decrease the TP of top consumers.

Exceptions to the trend of increasing TP with ontogeny were estimates of TP_{SCA} in the northern area and TP_{bulk} for adults in the southern area. TP_{SCA} depends on the relative mass proportions of prey categories and their respective TP (Cortés 1999). The dominance of teleost prey with a narrow range in TP may have flattened the ontogenetic TP_{SCA} pattern in the northern area. Observed differences in TP_{SCA} and TP_{bulk} were expected, as SCA may identify food items ingested by skipjack only up to 12 h prior to capture (Magnuson 1969), while complete isotopic incorporation for rapidly growing yellowfin muscle is ~6 mo (Graham 2007), which is a sound proxy for muscle of skipjack. Therefore, SCA data integrates diet over very short time periods and requires continuous sampling to capture seasonal shifts in diet composition, which are captured via isotope analysis given the multi-month isotopic incorporation rate of muscle tissue. The lower and highly variable TP_{bulk} observed in adults from the southern area diverged from $TP_{Glx-Lys}$, likely due to the presence of individuals with low $\delta^{15}N_{bulk}$ values in this group that were not in steady-state with the southern $\delta^{15}N$ baseline (Coletto et al. 2021).

$TP_{Glx-Phe}$ estimates were one trophic level lower than TP_{SCA}, TP_{bulk}, and $TP_{Glx-Lys}$. A similar result was reported for yellowfin tuna by Lorrain et al. (2015),

who suggested that a $TDF_{Glx-Phe}$ of ~7.6‰ may be too large. Nuche-Pascual et al. (2021) indicated that $TDF_{Glx-Phe}$ varies with dietary protein content and feeding regime in teleosts, and suggested the use of taxon-specific trophic-source TDF values. We used a lower $TDF_{Glx-Phe}$ of 5.7‰ to estimate $TP_{Glx-Phe}$ in skipjack based on a large compilation of marine teleosts (Bradley et al. 2015). If we assume estimates of $\beta_{Glx-Phe}$ (3.6 ± 0.5‰) are robust for phytoplankton-fueled pelagic food webs in the SWAO, then $TDF_{Glx-Phe}$ for skipjack must be even lower than 5.7‰. Similar to patterns in $\delta^{15}N_{bulk}$ discrimination (Trueman et al. 2005), Glx may experience less nitrogen isotope fractionation in rapidly growing skipjack, or alternatively there could be significant trophic-relative fractionation of Phe, which previous work estimates might be as large as 1.5‰ in bluefin tuna (Bradley et al. 2014).

5. CONCLUSIONS

This study provides new information on skipjack foraging and movement ecology in the SWAO. The productive southern area supports a high abundance of forage species and large skipjack feeding aggregations. AA $\delta^{15}N$ analysis allowed us to separate the effects of foraging across distinct isotopic baselines from changes in TP with ontogeny. The decrease in $\delta^{15}N_{Lys}$ and $\delta^{15}N_{Phe}$ values with increasing skipjack size indicate that fully mature individuals forage in lower latitudes and further offshore than their younger counterparts. Our study advances our understanding of the application of AA-CSIA in pelagic marine ecosystems, showing that Lys $\delta^{15}N$ values were a more reliable proxy than Phe for baseline $\delta^{15}N$ and that TP estimates based on differences in $\delta^{15}N$ values between Glx (trophic) and Lys (source) were more accurate than those derived from Glx and Phe. Stock management strategies should consider that the southern region supports dense aggregations of juvenile skipjack, which appear to use these areas seasonally to enhance growth. If non-selective fishing gear (e.g. purse seining) are used in the future due to economic pressures, monitoring will be critical to control the catch of a minimum size above the size of first maturity. Finally, we encourage future studies applying bulk tissue and AA $\delta^{15}N$ analyses to cover the entire latitudinal distribution of the species in the SWAO to provide enhanced insights into skipjack movement and stock connectivity in this region.

LITERATURE CITED

Andrade HA (2003) The relationship between the skipjack tuna (*Katsuwonus pelamis*) fishery and seasonal temperature variability in the south-western Atlantic. Fish Oceanogr 12:10–18

Andrade HA, Kinas PG (2004) Estimation of birthdates and catch-at-age using length frequency analysis (LFA), with application for skipjack tuna (*Katsuwonus pelamis*) caught in the Southwest Atlantic. ICES J Mar Sci 61:798–811

Ankenbrandt L (1985) Food habits of bait-caught skipjack tuna, *Katsuwonus pelamis*, from the southwestern Atlantic Ocean. Fish Bull 83:379–393

Benevenuti Soares JB, Monteiro-Neto C, Costa MR, Martins RRM and others (2019) Size structure, reproduction, and growth of skipjack tuna (*Katsuwonus pelamis*) caught by the pole-and-line fleet in the southwest Atlantic. Fish Res 212:136–145

Bernal D, Brill RW, Dickson KA, Shiels HA (2017) Sharing the water column: physiological mechanisms underlying species-specific habitat use in tunas. Rev Fish Biol Fish 27:843–880

Bradley CJ, Madigan DJ, Block BA, Popp BN (2014) Amino acid isotope incorporation and enrichment factors in Pacific bluefin tuna, *Thunnus orientalis.* PLOS ONE 9:e85818

Bradley CJ, Wallsgrove NJ, Choy CA, Drazen JC, Hetherington ED, Hoen DK, Popp BN (2015) Trophic position estimates of marine teleosts using amino acid compound specific isotopic analysis. Limnol Oceanogr Methods 13:476–493

Bugoni L, McGill RAR, Furness RW (2010) The importance of pelagic longline fishery discards for a seabird community determined through stable isotope analysis. J Exp Mar Biol Ecol 391:190–200

Castello JP, Habiaga RP (1989) The skipjack tuna fishery in southern Brazil. Col Vol Sci Pap ICCAT 30:6–19

Castello JP, Haimovici M, Odebrecht C, Vooren CM (1997) The continental shelf and slope. In: Seeliger U, Odebrecht C, Castello JP (eds) Subtropical convergence envi-

ronments: the coast and sea in the southwestern Atlantic. Springer Verlag, p 171–178

Caut S, Angulo E, Courchamp F (2009) Variation in discrimination factors ($\Delta^{15}N$ and $\Delta^{13}C$): the effect of diet isotopic values and applications for diet reconstruction. J Appl Ecol 46:443–453

Cayré P, Farrugio H (1986) Biologie de la reproduction du listao (*Katsuwonus pelamis*) de l'Océan Atlantique. Proc ICCAT Intl Skipjack Yr Prog 1:252–272

Choy CA, Popp BN, Hannides CCS, Drazen JC (2015) Trophic structure and food resources of epipelagic and mesopelagic fishes in the North Pacific Subtropical Gyre ecosystem inferred from nitrogen isotopic compositions. Limnol Oceanogr 60:1156–1171

Colette BC, Nauen CE (1983) FAO species catalogue. Scombrids of the world. An annotated and illustrated catalogue of tuna, mackerels, bonitos and related species known to date. FAO Fish Synop 125

Coletto JL, Pinho MP, Madureira LSP (2019) Operational oceanography applied to skipjack tuna (*Katsuwonus pelamis*) habitat monitoring and fishing in south-western Atlantic. Fish Oceanogr 28:82–93

Coletto JL, Fischer LG, Szepaniuk AW, Catelani PA, Botta S, Madureira LSP (2020) Trophic ecology of the skipjack tuna in the southeastern and southern regions of Brazil. In: Madureira LSP, Monteiro-Neto C (eds) Sustainability of skipjack tuna fishery in Brazil. Paco Editorial, Jundiaí, p 112–127

Coletto JL, Botta S, Fischer LG, Newsome SD, Madureira LSP (2021) Isotope-based inferences of skipjack tuna feeding ecology and movement in the southwestern Atlantic Ocean. Mar Environ Res 165:105246

Cortés E (1999) Standardized diet compositions and trophic levels of sharks. ICES J Mar Sci 56:707–717

Costa PL, Valderrama PRC, Madureira LSP (2016) Relationships between environmental features, distribution and abundance of the Argentine anchovy, *Engraulis anchoita*, on the south west Atlantic Continental Shelf. Fish Res 173:229–235

Costa PL, Bugoni L, Kinas PG, Madureira LASP (2020a) Seabirds, environmental features and the Argentine anchovy *Engraulis anchoita* in the southwestern Atlantic Ocean. Mar Ecol Prog Ser 651:199–213

Costa MR, Tubino RA, Castello JP, Mello VS and others (2020b) Life cycle knowledge of the skipjack tuna in the Southwest Atlantic. In: Madureira LSP, Monteiro-Neto C (eds) Sustainability of skipjack tuna fishery in Brazil. Paco Editorial, Jundiaí, p 79–93

Dale JJ, Wallsgrove NJ, Popp BN, Holland KN (2011) Nursery habitat use and foraging ecology of the brown stingray *Dasyatis lata* determined from stomach contents, bulk and amino acid stable isotopes. Mar Ecol Prog Ser 433:221–236

DeNiro MJ, Epstein J (1981) Influence of diet on the distribution of nitrogen isotopes in animals. Geochim Cosmochim Acta 45:341–351

FAO (2020) The state of world fisheries and aquaculture 2020. Sustainability in action. FAO, Rome

Figueiredo JL, Menezes NA (1980) Manual de peixes marinhos do sudeste do Brasil. III. Teleostei (2). Museu de Zoologia, Universidade de São Paulo

Garcia CAE (1997) Hydrographic characteristics. In: Seeliger U, Odebrecht C, Castello JP (eds) Subtropical convergence environments: the coast and sea in the Southwestern Atlantic. Springer Verlag, p 104–106

Gasalla MA, Velasco G, Rossi-Wongtschowski CLDB, Haimovici M, Madureira LSP (2007) Modelo de equilíbrio de biomassas do ecossistema marinho da Região Sudeste-Sul do Brasil entre 100–1000 m de profundidade. In: Rossi-Wongtschowski CLDB (ed), Série documentos Revizee: Score Sul, São Paulo, p 11–55

Gibbons MJ, Spiridonov VA, Tarling GA (1999) Euphausiacea. In: Boltovskoy D (ed) South Atlantic Zooplankton. Backhuys Publishers, Leiden, p 1241–1279

Gorri C (1995) Distribuição espaço-temporal e estrutura populacional de Euphausiacea (Crustacea) na região do extremo sul do Brasil (31° 40′ S–33° 45′ S). MSc dissertation, Federal University of Rio Grande

Graham BS (2007) Trophic dynamics and movements of tuna in the tropical Pacific Ocean inferred from stable isotope analyses. PhD dissertation, University of Hawaii at Manoa, Honolulu, HI

Graham BS, Grubbs D, Holland K, Popp BN (2007) A rapid ontogenetic shift in the diet of juvenile yellowfin tuna from Hawaii. Mar Biol 150:647–658

Graham BS, Koch PL, Newsome SD, McMahon KW, Aurioles D (2010) Using isoscapes to trace the movements and foraging behavior of top predators in oceanic ecosystems. In: West J, Bowen G, Dawson T, Tu K (eds) Isoscapes. Springer, Dordrecht, p 299–318

Haimovici M, Santos RA, Fischer LG (2009) Class Cephalopoda. In: Rios EC (ed) Compendium of Brazilian sea shells. Evangraf, Rio Grande, p 610–649

Hannides CCS, Popp BN, Landry MR, Graham BS (2009) Quantification of zooplankton trophic position in the North Pacific Subtropical Gyre using stable nitrogen isotopes. Limnol Oceanogr 54:50–61

Houssard P, Lorrain A, Tremblay-Boyer L, Allain V and others (2017) Trophic position increases with thermocline depth in yellowfin and bigeye tuna across the Western and Central Pacific Ocean. Prog Oceanogr 154:49–63

Jablonski S, Braile AA, Romao CM, Teixeira MSM (1984) Sexual maturity and sex ratios of the skipjack tuna, *Katsuwonus pelamis* (Linnaeus), from Southeastern Brazil. Col Vol Sci Pap ICCAT 20:217–233

Katsuragawa M, dos Santos ESLG, Namiki CAP, Zani-Teixeira ML, Matsuura Y (2020) Life cycle phases of the skipjack tuna on the Brazilian coast. In: Madureira LSP, Monteiro-Neto C (eds) Sustainability of skipjack tuna fishery in Brazil. Paco Editorial, Jundiaí, p 70–78

Kiyofuji H, Aoki Y, Kinoshita J, Okamoto S and others (2019) Northward migration dynamics of skipjack tuna (*Katsuwonus pelamis*) associated with the lower thermal limit in the western Pacific Ocean. Prog Oceanogr 175:55–67

Le-Alvarado M, Romo-Curiel AE, Sosa-Nishizaki O, Hernández-Sánchez O, Barbero L, Herzka SZ (2021) Yellowfin tuna (*Thunnus albacares*) foraging habitat and trophic position in the Gulf of Mexico based on intrinsic isotope tracers. PLOS ONE 16:e0246082

Lima JHM, Lin CF, Menezes AAS (2000) A description of the baitboat fishery off the south and southeast Brazil. Col Vol Sci Pap ICCAT 51:416–462

Lorrain A, Graham BS, Popp BN, Allain V and others (2015) Nitrogen isotopic baselines and implications for estimating foraging habitat and trophic position of yellowfin tuna in the Indian and Pacific Oceans. Deep Sea Res II 113:188–198

Luckhurst BE (2014) Elements of the ecology and movement patterns of highly migratory fish species of interest to

ICCAT in the Sargasso Sea. Col Vol Sci Pap ICCAT 70: 2183–2206

Madigan DJ, Litvin SY, Popp BN, Carlisle AB, Farwell CJ, Block BA (2012) Tissue turnover rates and isotopic trophic discrimination factors in the endothermic teleost, Pacific bluefin tuna (*Thunnus orientalis*). PLOS ONE 7: e49220

Madigan DJ, Baumann Z, Carlisle AB, Hoen DK and others (2014) Reconstructing transoceanic migration patterns of Pacific bluefin tuna using a chemical tracer toolbox. Ecology 95:1674–1683

Madigan DJ, Chiang WC, Wallsgrove NJ, Popp BN and others (2016) Intrinsic tracers reveal recent foraging ecology of giant Pacific bluefin tuna at their primary spawning grounds. Mar Ecol Prog Ser 553:253–266

Madureira LSP, Vasconcellos MC, Weigert SC, Habiaga RP and others (2005) Distribuição, abundância e interações ambientais de espécies pelágicas na Região Sudeste-Sul do Brasil, entre o Cabo de São Tomé (RJ) e o Chuí (RS). In: Madureira LSP, Rossi-Wongtschowski CLDB (eds) Prospecção de recursos pesqueiros pelágicos na Zona Economica Exclusiva da Região Sudeste-Sul do Brasil: hidroacústica e biomassas. Série de Documentos REVIZEE-SCORE SUL, São Paulo, p 63–126

Madureira LSP, Castello JP, Prentice-Hernández C, Queiroz MI and others (2009) Current and potential alternative food uses of the Argentine anchoita (*Engraulis anchoita*) in Argentina, Uruguay and Brazil. In: Hasan MR, Halwart M (eds) Fish as feed inputs for aquaculture: practices, sustainability and implications. FAO Fish Tech Pap 518:269–287

Magnuson JJ (1969) Digestion and food consumption by skipjack tuna (*Katsuwonus pelamis*). Trans Am Fish Soc 98:379–392

Marques FP, Cardoso LG, Haimovici M, Bugoni L (2018) Trophic ecology of Magellanic penguins (*Spheniscus magellanicus*) during the non-breeding period. Estuar Coast Shelf Sci 210:109–122

Matsuura Y, Andrade HA (2000) Synopsis on biology of skipjack tuna population and related environmental conditions in Brazilian waters. Col Vol Sci Pap ICCAT 51: 395–400

McClelland JW, Montoya JP (2002) Trophic relationships and the nitrogen isotopic composition of amino acids in plankton. Ecology 83:2173–2180

McCutchan JHJ, Lewis WM, Kendall C, McGrath CC (2003) Variation in trophic shift for stable isotope ratios of carbon, nitrogen, and sulfur. Oikos 102:378–390

McMahon KW, McCarthy MD (2016) Embracing variability in amino acid δ^{15}N fractionation: mechanisms, implications, and applications for trophic ecology. Ecosphere 7: e01511

McMahon KW, Newsome SD (2019) Amino acid isotope analysis: a new frontier in studies of animal migration and foraging ecology. In: Hobson KA, Wassenaar LI (eds) Tracking animal migration with stable isotopes. Academic Press, p 173–190

McMahon KW, Hamady LL, Thorrold SR (2013) A review of ecogeochemistry approaches to estimating movements of marine animals. Limnol Oceanogr 58:697–714

Médieu A, Point D, Receveur A, Gauthier O and others (2021) Stable mercury concentrations of tropical tuna in the south western Pacific ocean: an 18-year monitoring study. Chemosphere 263:128024

Ménard F, Lorrain A, Potier M, Marsac F (2007) Isotopic evi-
dence of distinct feeding ecologies and movement patterns in two migratory predators (yellowfin tuna and swordfish) of the western Indian Ocean. Mar Biol 153: 141–152

Minagawa M, Wada E (1984) Stepwise enrichment of ^{15}N along food chains: further evidences and the relation between δ^{15}N and animal age. Geochim Cosmochim Acta 48:1135–1140

Monteiro-Neto C, Costa MR, Tubino RA, Macena BC, Madureira LSP, Pinho M (2020) Use of electronic tags for identification of skipjack tuna movement patterns. In: Madureira LSP, Monteiro-Neto C (eds) Sustainability of skipjack tuna fishery in Brazil. Paco Editorial, Jundiaí, p 50–68

Murua H, Rodriguez-Marin E, Neilson JD, Farley JH, Juan-Jordá MJ (2017) Fast versus slow growing tuna species: age, growth, and implication for population dynamics and fisheries management. Rev Fish Biol Fish 27:733–773

Nuche-Pascual MT, Ruiz-Cooley RI, Herzka SZ (2021) A meta-analysis of amino acid δ^{15}N trophic enrichment factors in fishes relative to nutritional and ecological drivers. Ecosphere 12:e03570

Olson RJ, Popp BN, Graham BS, Lópes-Ibarra GA and others (2010) Food-web inferences of stable isotope spatial patterns in copepods and yellowfin tuna in the pelagic eastern Pacific Ocean. Prog Oceanogr 86:124–138

Parnell A (2019) simmr: a stable isotope mixing model. R package version 0.4.1. https://CRAN.R-project.org/package=simmr

Peterson BJ, Fry B (1987) Stable isotopes in ecosystem studies. Annu Rev Ecol Syst 18:293–320

Pethybridge H, Choy CA, Logan JM, Allain V and others (2018) A global meta-analysis of marine predator nitrogen stable isotopes: relationships between trophic structure and environmental conditions. Glob Ecol Biogeogr 27:1043–1055

Popp BN, Graham BS, Olson RJ, Hannides CCS and others (2007) Insight into the trophic ecology of yellowfin tuna, *Thunnus albacares*, from compound-specific nitrogen isotope analysis of proteinaceous amino acids. In: Dawson TD, Siegwolf TRW (eds) Stable isotopes as indicators of ecological change. Elsevier/Academic Press, Terrestrial Ecology Series, San Diego, CA, p 173–190

Post DM (2002) Using stable isotopes to estimate trophic position: models, methods, and assumptions. Ecology 83: 703–718

Post DM, Layman CA, Arrington DA, Takimoto G, Quattrochi J, Montaña CG (2007) Getting to the fat of the matter: models, methods and assumptions for dealing with lipids in stable isotope analyses. Oecologia 152:179–189

Quezada-Romegialli C, Jackson AL, Harrod C (2019) tRophic Position: Bayesian trophic position calculation with stable isotopes. R package version 0.7.7. https://cran.r-project.org/web/packages/tRophicPosition/tRophicPosition.pdf

R Core Team (2019) R: a language and environment for statistical computing. R Foundation for Statistical Computing, Vienna

Revill AT, Young JW, Lansdell M (2009) Stable isotopic evidence for trophic groupings and bio-regionalization of predators and their prey in oceanic waters off eastern Australia. Mar Biol 156:1241–1253

Sabadel AJM, Durante LM, Wing SR (2020) Stable isotopes of amino acids from reef fishes uncover Suess and nitrogen enrichment effects on local ecosystems. Mar Ecol Prog Ser 647:149–160

Schaefer KM, Fuller DW (2013) Simultaneous behavior of skipjack (*Katsuwonus pelamis*), bigeye (*Thunnus obesus*), and yellowfin (*T. albacares*) tunas, within large multi-species aggregations associated with drifting fish aggregating devices (FADs) in the equatorial eastern Pacific Ocean. Mar Biol 160:3005−3014

Schaefer KM, Fuller DW, Block BA (2009) Vertical movements and habitat utilization of skipjack (*Katsuwonus pelamis*), yellowfin (*Thunnus albacares*), and bigeye (*Thunnus obesus*) tunas in the equatorial eastern Pacific Ocean, ascertained through archival tag data. In: Nielsen JL, Arrizabalaga H, Fragoso N, Hobday A, Lutcavage M, Sibert J (eds) Tagging and tracking of marine animals with electronic devices. Reviews: methods and technologies in fish biology and fisheries, Vol 9. Springer, Dordrecht, p 121−144

Sigman DM, Karsh KL, Casciotti KL (2009) Ocean process tracers: nitrogen isotopes in the ocean. In: Steele JH, Turekian KK, Thorpe SA (eds) Encyclopedia of ocean sciences, 2nd edn. Elsevier, Amsterdam, p 40−54

Silfer JA, Engel MH, Macko SA, Jumeau EJ (1991) Stable carbon isotope analysis of amino acid enantiomers by conventional isotope ratio mass spectrometry and combined gas chromatography/isotope ratio mass spectrometry. Anal Chem 63:370−374

Sogawa S, Sugisaki H, Tadokoro K, Ono T, Sato E, Shimode S, Kikuchi T (2017) Feeding habits of six species of euphausiids (Decapoda: Euphausiacea) in the northwestern Pacific Ocean determined by carbon and nitrogen stable isotope ratios. J Crustac Biol 37:29−36

Troina GC, Dehairs F, Botta S, Di Tullio JC, Elsken M, Secchi ER (2020a) Zooplankton-based δ^{13}C and δ^{15}N isoscapes from the outer continental shelf and slope in the subtropical western South Atlantic. Deep Sea Res I 159:103235

Troina GC, Botta S, Dehairs F, Di Tullio JC, Elskens M, Secchi ER (2020b) Skin δ^{13}C and δ^{15}N reveal spatial and temporal patterns of habitat and resource use by free-ranging odontocetes from the southwestern Atlantic Ocean. Mar Biol 167:186

Troina GC, Riekenberg P, van der Meer MTJ, Botta S, Dehairs F, Secchi ER (2021) Combining isotopic analysis of bulk-skin and individual amino acids to investigate the trophic position and foraging areas of multiple cetacean species in the western South Atlantic. Environ Res 201:111610

Trueman CN, Glew KSJ (2019) Isotopic tracking of marine animal movement. In: Hobson KA, Wassenaar LI (eds) Tracking animal migration with stable isotopes. Academic Press, London, p 137−172

Trueman CN, McGil RAR, Guyard PH (2005) The effect of growth rate on tissue−diet isotopic spacing in rapidly growing animals. An experimental study with Atlantic salmon (*Salmo salar*). Rapid Commun Mass Spectrom 19: 3239−3247

Vanderklift MA, Ponsard S (2003) Sources of variation in consumer-diet δ^{15}N enrichment: a meta-analysis. Oecologia 136:169−182

Vaske T Jr, Vooren CM, Lessa RP (2004) Feeding habits of four species of Istiophoridae (Pisces: Perciformes) from Northeastern Brazil. Environ Biol Fishes 70: 293−304

Velasco G, Castello JP (2005) An ecotrophic model of southern Brazil continental shelf and fisheries scenarios for *Engraulis anchoita* (Pisces, Engraulididae). Atlântica 27: 59−68

Vilela MJA (1990) Idade, crescimento, alimentação e avaliação do estoque de bonito listado, *Katsuwonus pelamis* (Scombridae: Thunnini), explorado na região sudeste — sul do Brasil. MSc dissertation, Universidade Federal do Rio Grande

Vilela MJA, Castello JP (1993) Dinamica poblacional del barrilete (*Katsuwonus pelamis*) explotado en la region sudeste — sur del Brasil em el período 1980−1986. Frente Marítimo 14:111−124

Whiteman JP, Elliott-Smith EA, Besser AC, Newsome SD (2019) A guide to using compound-specific stable isotope analysis to study the fates of molecules in organisms and ecosystems. Diversity (Basel) 11:8